Science Advances
AAAS

Supplementary Materials for

Multi-omics analysis reveals that linoleic acid metabolism is associated with variations of trained immunity induced by distinct BCG strains

Jin-Chuan Xu *et al.*

Corresponding author: Xiao-Yong Fan, xyfan008@fudan.edu.cn; Shui-hua Lu, lushuihua66@126.com; Zhidong Hu, huzhidong@fudan.edu.cn

Sci. Adv. **10**, eadk8093 (2024)
DOI: 10.1126/sciadv.adk8093

The PDF file includes:

Figs. S1 to S7
Legends for tables S1 to S6

Other Supplementary Material for this manuscript includes the following:

Tables S1 to S6

Supplementary figures

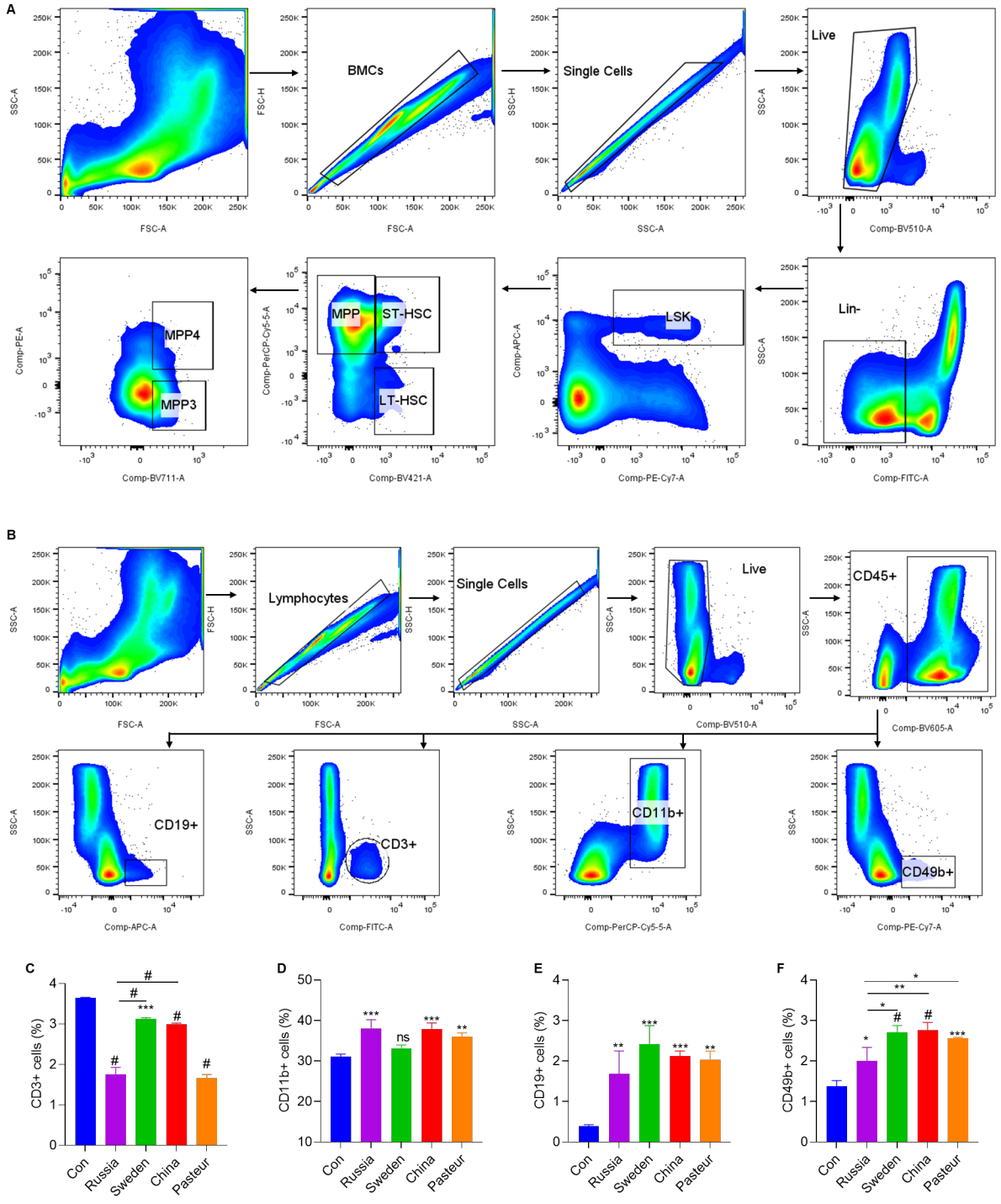

Figure S1. BCGs vaccination induced central and peripheral immunological modifications. (**A**). Cells were gated for FSC-A against SSC-A. Doublets were excluded using FSC-H against FSC-A and SSC-H against SSC-A. Viable cells were

gated. Within the lineage-negative population (BV510-), cells were gated as LSK- defined as double positive for cKit (FITC) and Sca-1 (APC). Gated on the LSK population, cells were divided into LT-HSC, ST-HSC and MPP based on CD150 (BV421) and CD48 (PerCP-Cy5.5) expression. MPPs were characterized as MPP3 or MPP4 by their surface expression of CD34 (BV711) and Flt3 (PE). (**B**). Cells were gated for FSC-A against SSC-A. Doublets were excluded using FSC-H against FSC-A and SSC-H against SSC-A. Viable cells were gated. Within the $CD45^+$ population, cells were gated as $CD19^+$ cells (APC), $CD3^+$ cells (FITC), $CD11b^+$ cells (PerCP-Cy5.5) and $CD49b^+$ cells (PE-Cy7). (**C**). Proportion of $CD3^+$ cells in $CD45^+$ cells. (**D**). Proportion of $CD11b^+$ cells in $CD45^+$ cells. (**E**). Proportion of CD19+ cells in $CD45^+$ cells. (**F**). Proportion of $CD49b^+$ cells in $CD45^+$ cells. One-way ANOVA test was used to compare groups, *ns*, not significant; $*P < 0.05$; $**P < 0.01$; $***P < 0.001$; $^{\#}P < 0.0001$. Data represent mean ± SD of three independent biological duplicates.

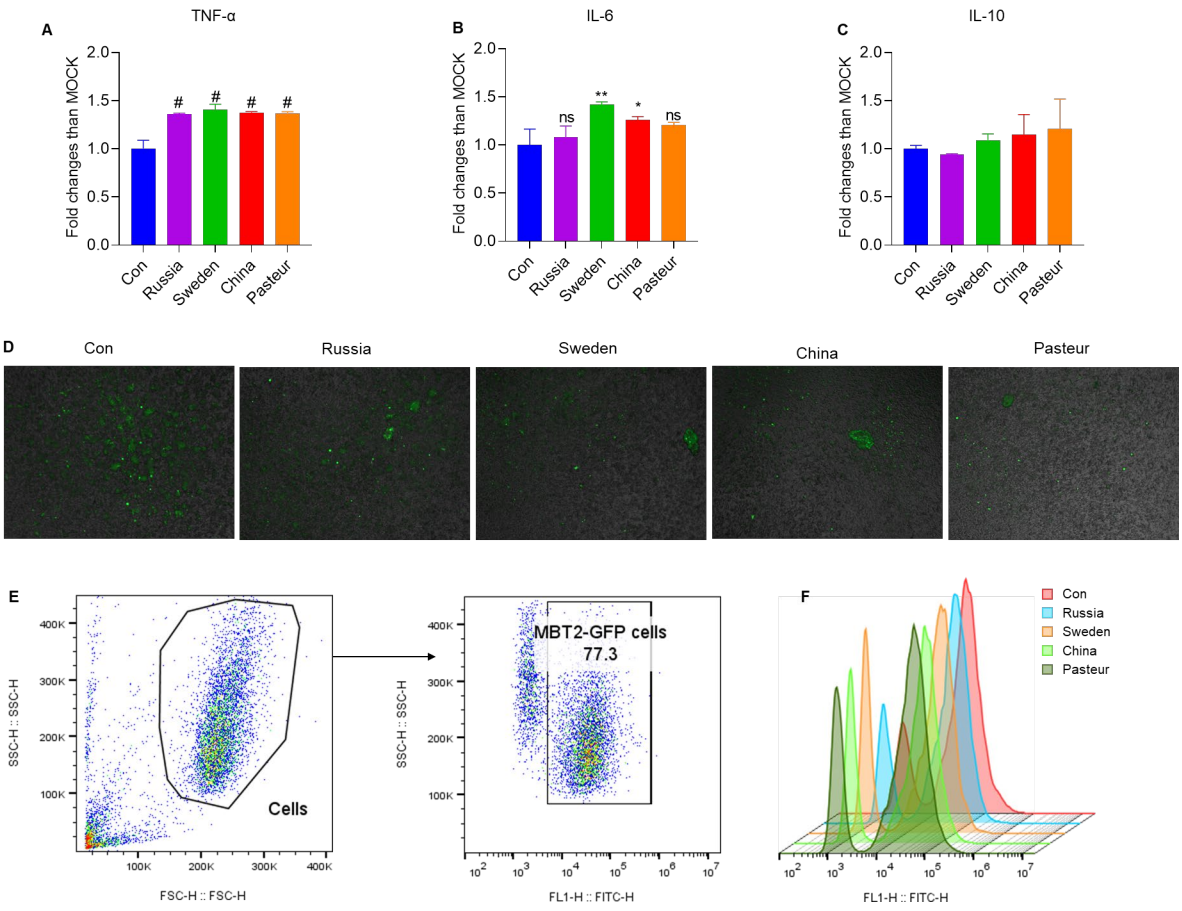

Figure S2. BCGs training provided non-specific protection. (**A-C**). Cytokine profiles of BMDMs post 24 h training. Data represent mean ± SD of three independent biological duplicates. One-way ANOVA test was used to compare groups, ns, not significant; *$P < 0.05$; **$P < 0.01$; ***$P < 0.001$; $^{\#}P < 0.0001$. (**D**). Proliferation of MBT2-GFP cells co-cultured with BCG trained BMDM cells. (**E**). Gating strategy for MBT2-GFP detection. (**F**). Histogram of proportion of MBT2-GFP cells co-cultured with BCG trained BMDMs.

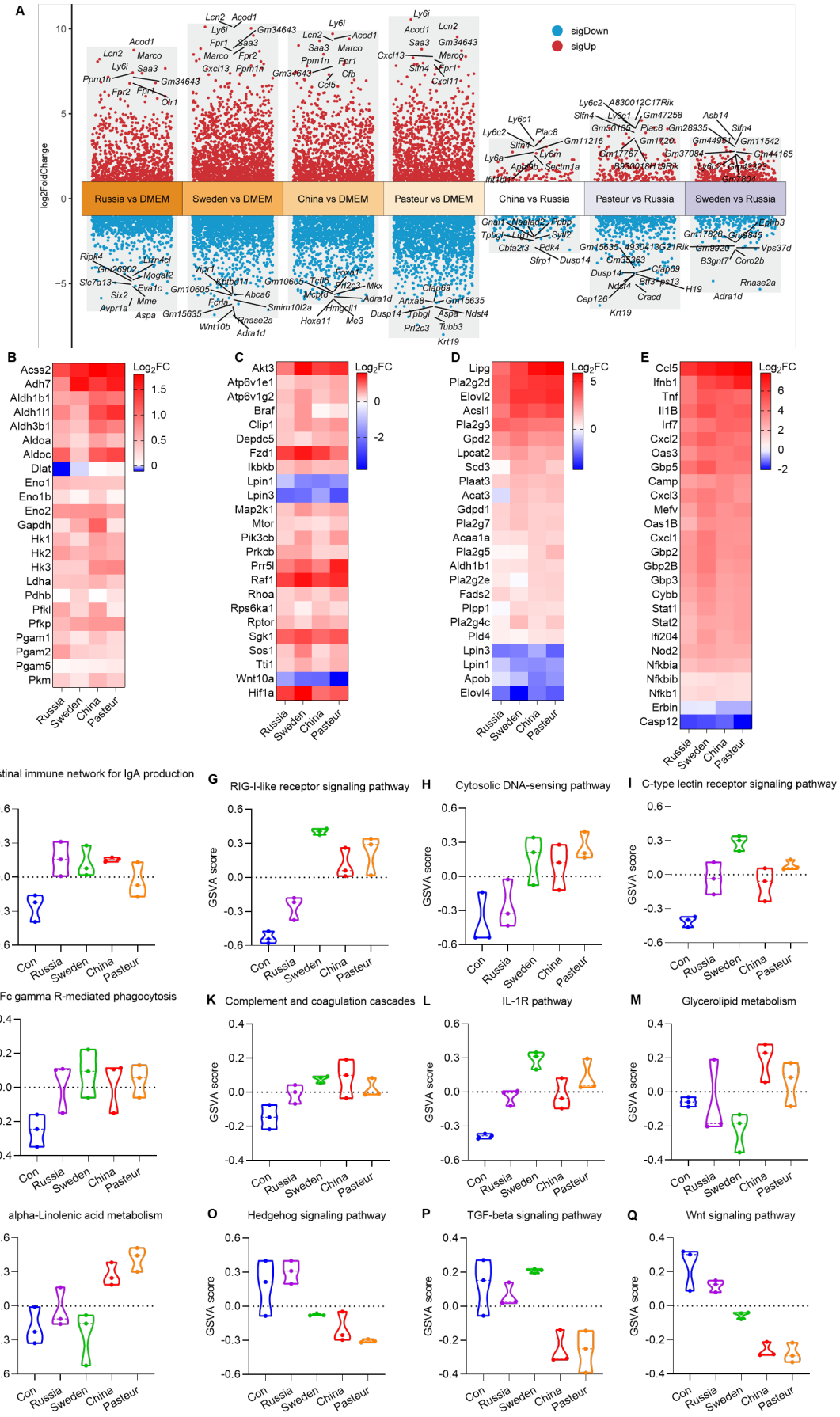
A
log2FoldChange
sigDown
sigUp
Russia vs DMEM
Sweden vs DMEM
China vs DMEM
Pasteur vs DMEM
China vs Russia
Pasteur vs Russia
Sweden vs Russia
B
C
D
E
Log2FC
Russia
Sweden
China
Pasteur
F Intestinal immune network for IgA production
G RIG-I-like receptor signaling pathway
H Cytosolic DNA-sensing pathway
I C-type lectin receptor signaling pathway
J Fc gamma R-mediated phagocytosis
K Complement and coagulation cascades
L IL-1R pathway
M Glycerolipid metabolism
N alpha-Linolenic acid metabolism
O Hedgehog signaling pathway
P TGF-beta signaling pathway
Q Wnt signaling pathway
GSVA score
Con
Russia
Sweden
China
Pasteur

Figure S3. Transcription profiles of BCGs-trained BMDM cells. (**A**). Volcano plots of DEGs. (**B**). Heatmap of genes involved in glycolysis metabolism. (**C**). Heatmap of genes involved in Akt-mtor-hif1a axis. (**D**). Heatmap of genes involved in lipid metabolism. (**E**). Heatmap of genes involved in NOD-like receptor signaling pathway. (**F-L**). Violin plots of the GSVA analysis involved in cell activation and inflammation. (**M**). Violin plots of the GSVA analysis of glycerolipid metabolism. (**N**). Violin plots of the GSVA analysis of alpha-linoleic acid metabolism. (**O**). Violin plots of the GSVA analysis of hedgehog signaling pathway. (**P**). Violin plots of the GSVA analysis of TGF-beta signaling pathway. (**Q**). Violin plots of the GSVA analysis of Wnt signaling pathway. Data represent mean ± SD of three independent biological duplicates.

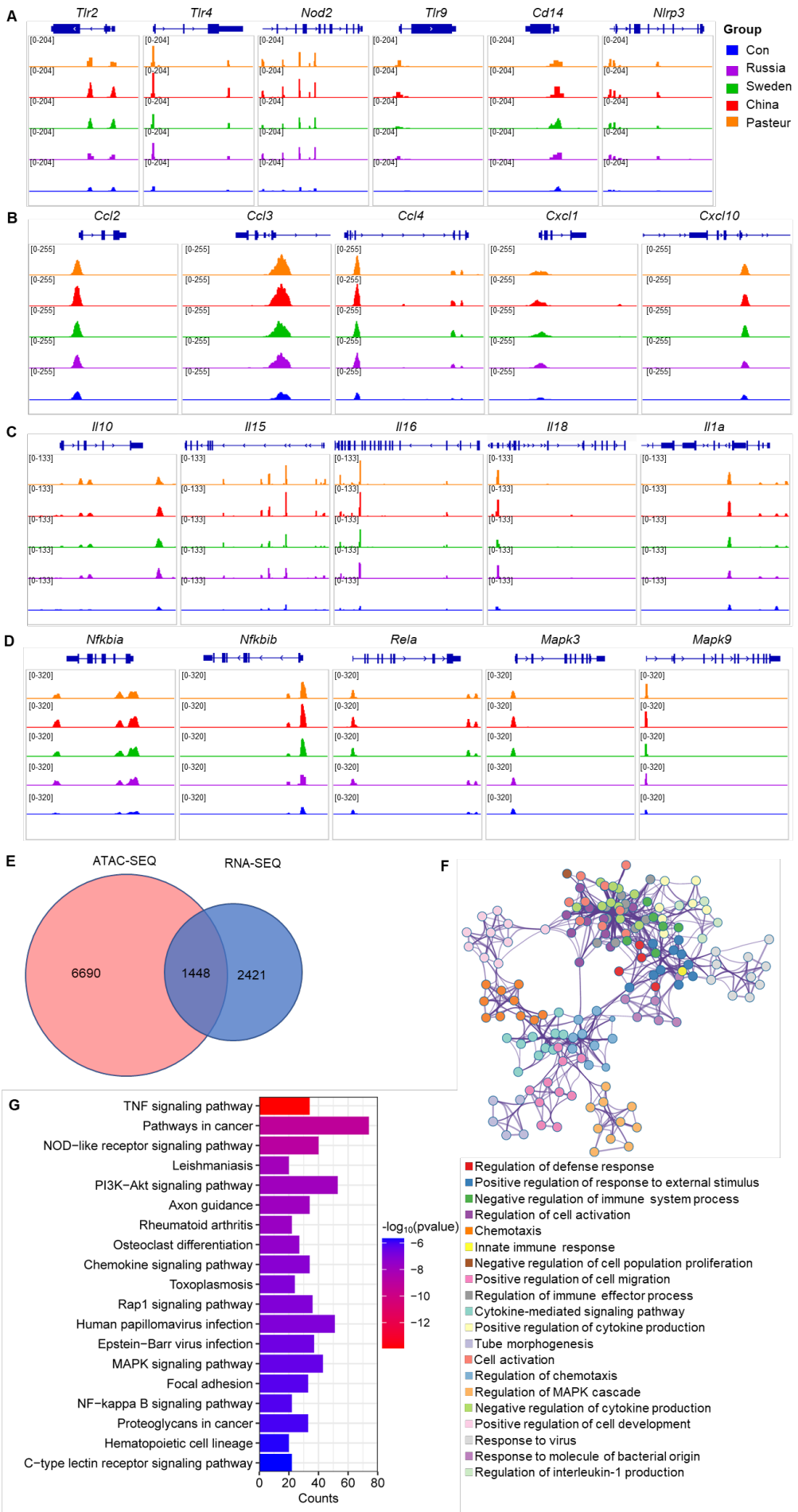
A
Tlr2
Tlr4
Nod2
Tlr9
Cd14
Nlrp3
Group
Con
Russia
Sweden
China
Pasteur
B
Ccl2
Ccl3
Ccl4
Cxcl1
Cxcl10
C
Il10
Il15
Il16
Il18
Il1a
D
Nfkbia
Nfkbib
Rela
Mapk3
Mapk9
E
ATAC-SEQ
RNA-SEQ
6690
1448
2421
F
Regulation of defense response
Positive regulation of response to external stimulus
Negative regulation of immune system process
Regulation of cell activation
Chemotaxis
Innate immune response
Negative regulation of cell population proliferation
Positive regulation of cell migration
Regulation of immune effector process
Cytokine-mediated signaling pathway
Positive regulation of cytokine production
Tube morphogenesis
Cell activation
Regulation of chemotaxis
Regulation of MAPK cascade
Negative regulation of cytokine production
Positive regulation of cell development
Response to virus
Response to molecule of bacterial origin
Regulation of interleukin-1 production
G
TNF signaling pathway
Pathways in cancer
NOD−like receptor signaling pathway
Leishmaniasis
PI3K−Akt signaling pathway
Axon guidance
Rheumatoid arthritis
Osteoclast differentiation
Chemokine signaling pathway
Toxoplasmosis
Rap1 signaling pathway
Human papillomavirus infection
Epstein−Barr virus infection
MAPK signaling pathway
Focal adhesion
NF−kappa B signaling pathway
Proteoglycans in cancer
Hematopoietic cell lineage
C−type lectin receptor signaling pathway
0
20
40
60
80
Counts
-log10(pvalue)
−6
−8
−10
−12

Figure S4. Epigenetic profiles of BCGs-trained BMDM cells. (**A**). Bar chart of ATAC signal in inflammatory receptors genes. (**B**). Bar chart of ATAC signal in chemokines genes. (**C**). Bar chart of ATAC signal in cytokines genes. (**D**). Bar chart of ATAC signal in NOD-like receptor signal pathway genes. (**E**). Veen diagram of pooled DEGs in RNA-seq and pooled DAGs in ATAC-seq. (**F**). Networks of GOBP enrichment analysis of 1448 intersection genes in E. (**G**). Top 20 KEGG pathways of 1448 intersection genes in E.

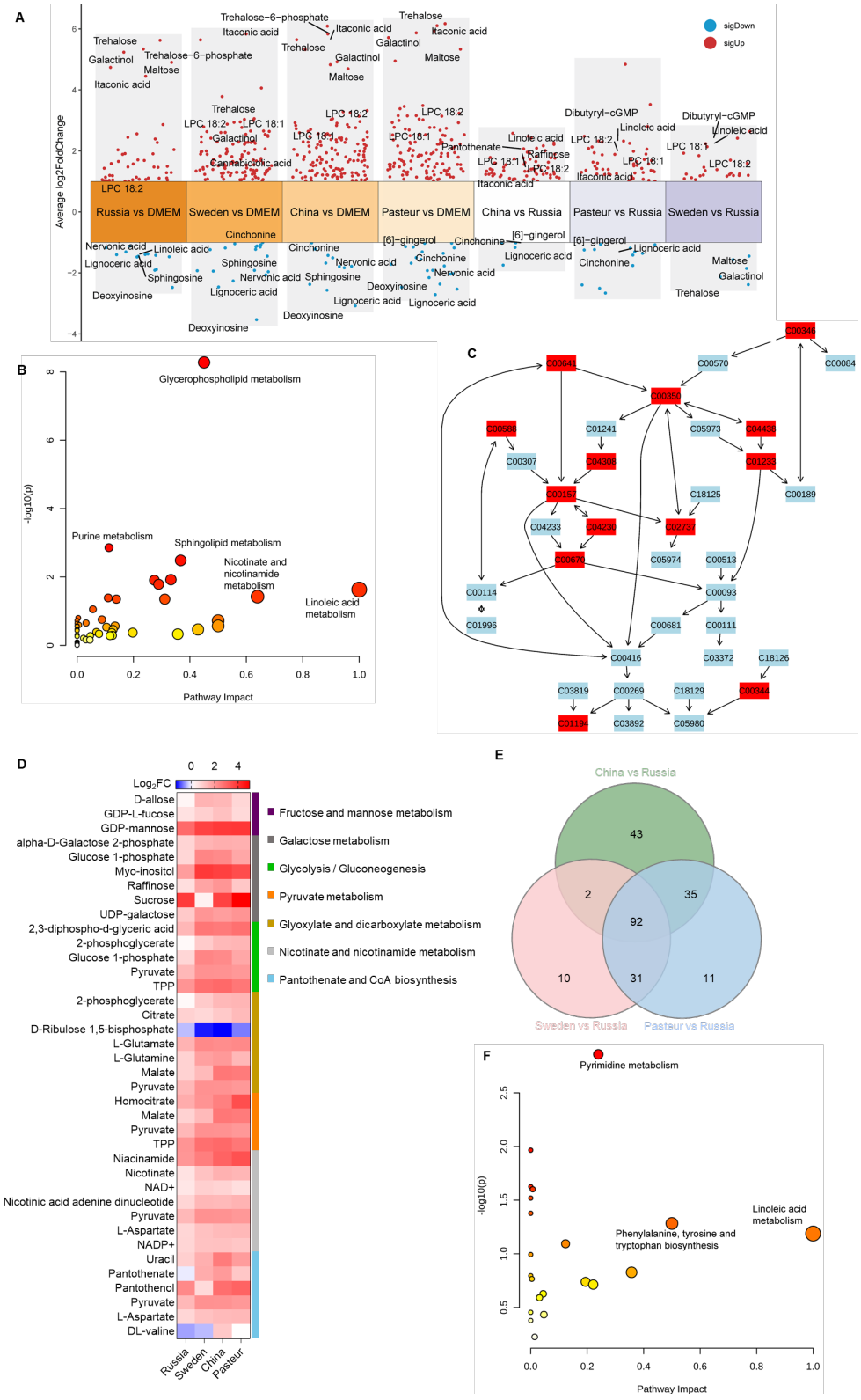

Figure S5. Metabolic profiles of BCGs-trained BMDM cells. (**A**). Volcano plots of differentially metabolites. (**B**). KEGG pathway analysis of pooled DMs. (**C**). Glycerophospholipid metabolism pathway mapping of the involved metabolites. (**D**). Heatmap of DMs involved in Carbohydrate metabolism and Metabolism of cofactors and vitamins. (**E**). Venn diagram of differential metabolites in Sweden vs Russia, China vs Russia and Pasteur vs Russia groups. (**F**). KEGG pathway analysis of 43 DMs in E.

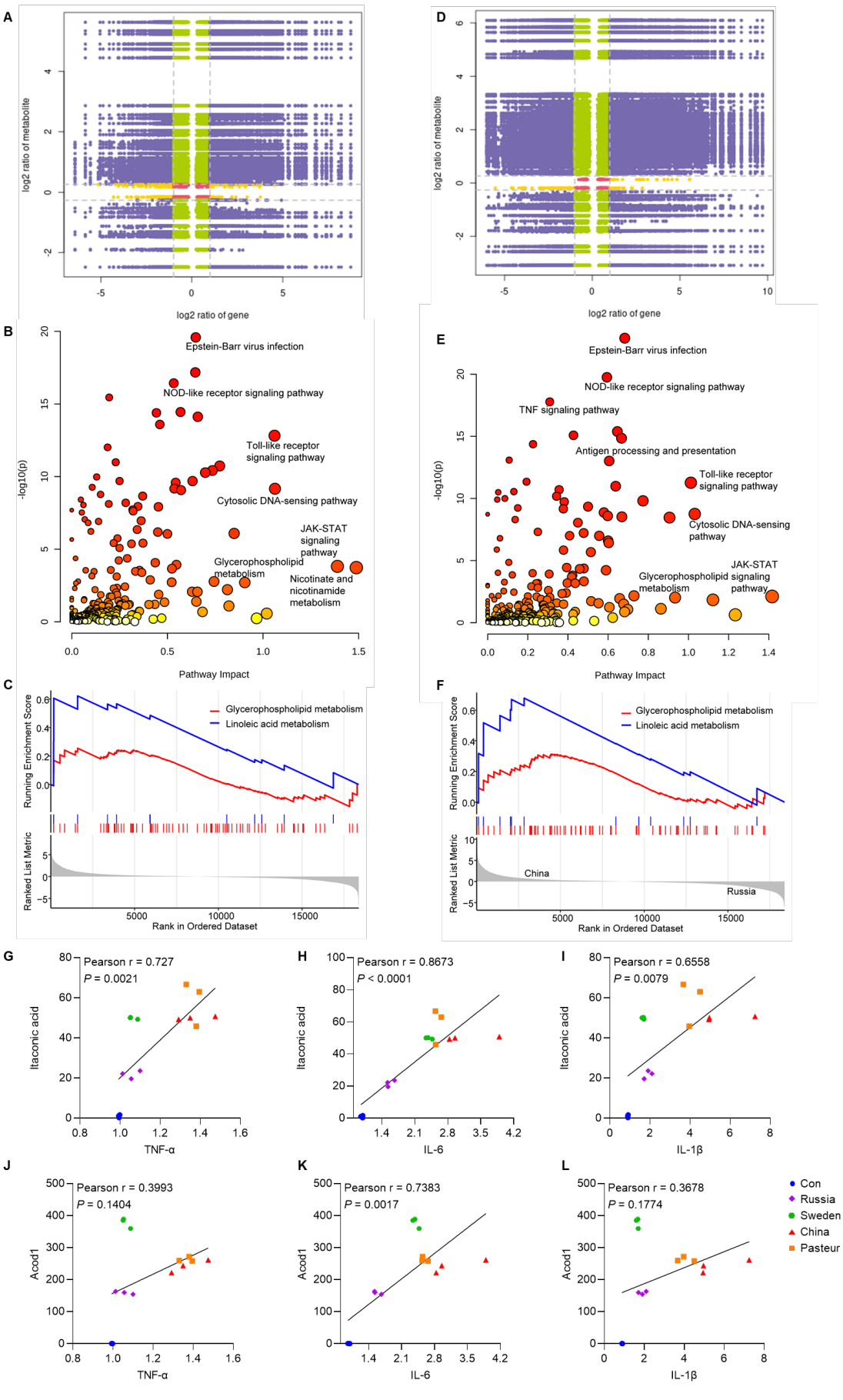
A
log2 ratio of metabolite
log2 ratio of gene
D
log2 ratio of metabolite
log2 ratio of gene
B
-log10(p)
Epstein-Barr virus infection
NOD-like receptor signaling pathway
Toll-like receptor signaling pathway
Cytosolic DNA-sensing pathway
JAK-STAT signaling pathway
Glycerophospholipid metabolism
Nicotinate and nicotinamide metabolism
Pathway Impact
E
-log10(p)
Epstein-Barr virus infection
NOD-like receptor signaling pathway
TNF signaling pathway
Antigen processing and presentation
Toll-like receptor signaling pathway
Cytosolic DNA-sensing pathway
JAK-STAT signaling pathway
Glycerophospholipid metabolism
Pathway Impact
C
Running Enrichment Score
Glycerophospholipid metabolism
Linoleic acid metabolism
Ranked List Metric
Rank in Ordered Dataset
F
Running Enrichment Score
Glycerophospholipid metabolism
Linoleic acid metabolism
Ranked List Metric
China
Russia
Rank in Ordered Dataset
G
Pearson r = 0.727
P = 0.0021
Itaconic acid
TNF-α
H
Pearson r = 0.8673
P < 0.0001
Itaconic acid
IL-6
I
Pearson r = 0.6558
P = 0.0079
Itaconic acid
IL-1β
J
Pearson r = 0.3993
P = 0.1404
Acod1
TNF-α
K
Pearson r = 0.7383
P = 0.0017
Acod1
IL-6
L
Pearson r = 0.3678
P = 0.1774
Acod1
IL-1β
Con
Russia
Sweden
China
Pasteur

Figure S6. Combined analysis of DMs with DEGs and cytokines. (**A**). Nine quadrant chart of mRNA expression ratios and metabolite expression ratios in Russia vs Con group [purple dots, significant changes in both metabolite and mRNA; green dots, significant changes in metabolite only; yellow dots, significant changes in mRNA only]. (**B**). Integrated analysis of metabolites and genes in part 3 of A. (**C**). GSEA enrichment plot of the KEGG glycerophospholipid metabolism and linoleic acid metabolism pathway of Russia vs Con. (**D**). Nine quadrant chart of mRNA expression ratios and metabolite expression ratios in China vs Con group [purple dots, significant changes in both metabolite and mRNA; green dots, significant changes in metabolite only; yellow dots, significant changes in mRNA only]. (**E**). Integrated analysis of metabolites and genes in part 3 of D. (**F**). GSEA enrichment plot of the KEGG glycerophospholipid metabolism and linoleic acid metabolism pathway of China vs Con. (**G**). Correlation between TNF-α fold change and itaconic acid fold change. (**H**). Correlation between IL-6 fold change and itaconic acid fold change. (**I**). Correlation between IL-1β fold change and itaconic acid fold change. (**J**). Correlation between TNF-α fold change and Acod1 expression. (**K**). Correlation between IL-6 fold change and Acod1 expression. (**L**). Correlation between IL-1β fold change and Acod1 expression.

A

Group	OD600	Suspension volume	Final volume	Injection volume	Bacterial counts
Russia	0.242	16.5 μL	2 mL	30 μL	6634
Sweden	0.257	15.6 μL	2 mL	30 μL	6465
China	0.259	15.4 μL	2 mL	30 μL	6386
Pasteur	0.254	15.7 μL	2 mL	30 μL	6321

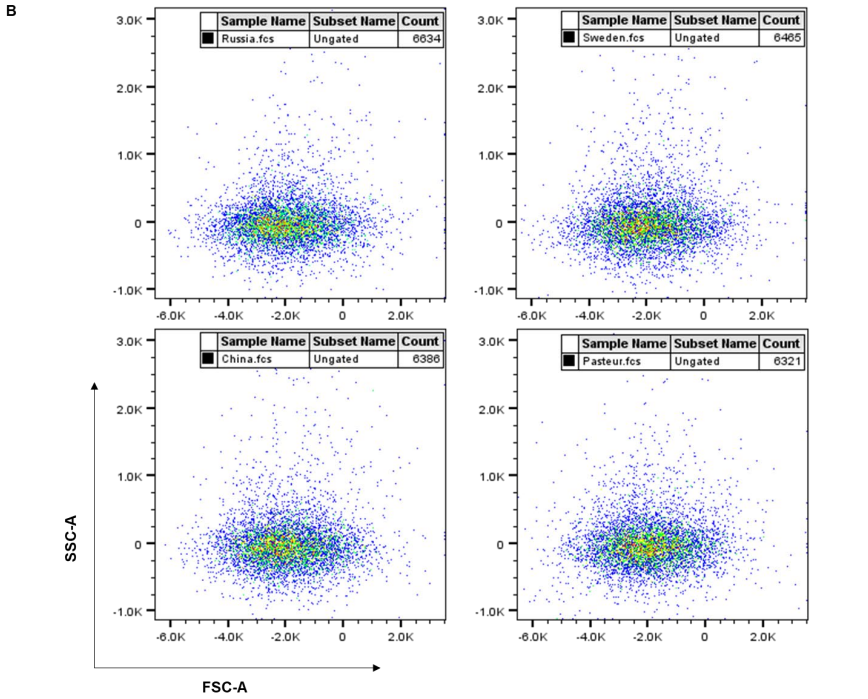

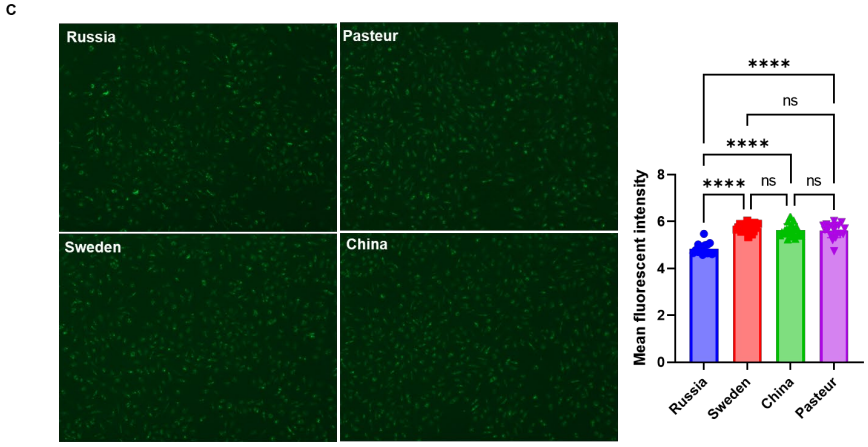

Figure S7. BCG single bacteria suspension preparation and intake experiment. (**A**). Parameters for flow cytometry detection of BCG suspension. Different BCG single bacterial suspensions were measured for OD_{600} and then adjusted to similar OD_{600} values (Concentration: $OD_{600}\times1\times10^8$/mL), and then a similar volume (suspension volume) was taken into the desired DMEM/F12 medium (Final volume: 2mL) to obtain a single bacterial suspension for training (approximately 6×10^4 bacteria in 300μL). The concentration of the number of bacteria (about 6×10^3 bacteria in 30μL) was determined by flow cytometry analysis of the fixed volume (injection volume: 30μL). (**B**). Representative flow cytometry plot of four BCG strains suspension (30μL). (**C**). BCG intake of macrophages after 24 h training. BMDMs were infected with BCG (MOI = 1) for 24 hours and then stained for intracellular bacteria with Auramine O, then photographed by fluorescence microscopy and quantified by ImageJ.

Table S1. GOBP enrichment analysis of 1338 intersection genes shared by the four groups in Figure 4C.

Table S2. Differential ATAC peak distributions on gene loci.

Table S3. GOBP enrichment analysis of 2146 intersection genes shared by the four groups in Figure 5D.

Table S4. GOBP and KEGG enrichment analysis of 1448 intersection genes in Figure S4E.

Table S5. DMs in Figure 6D.

Table S6. DMs in Figure 6E.